Supplementary information

Supplementary methods, Supplementary References, Supplementary Figures S1 to S4 and Supplementary Table S1 (strain list)

Supplementary methods

Figure S1. FISH was performed on paraformaldehyde fixed cells as described [S1]. Cosmids were used as FISH probes. Chromosome 1 cosmids were obtained from the Sanger Sanger (U. K.) and used as in [S1]. Chromosome 2 cosmids used as probes were c1228 (cen2 proximal) and c3F8 (left arm) [S2]. Distances between FISH signals were measured from maximum projections of images created from z series of eight 0.4-µm steps using MetaMorph software.

Figure S2 and S3. Pds5-GFP was detected using anti-GFP polyclonal antibodies (A11122, 2µg/µl) on nuclear spreads (D800) and by ChiP (2µg/ChiP).

Figure S4. Cells were arrested in G1 by the overexpression of a C-terminal fragment of the Res1 protein as described [S3]. To estimate Rad21 half-life on chromatin, individual data sets were fitted to a single exponential function using GraphPadPrism 4 (GraphPad Software).

Supplementary References

S1. Bernard P, Maure JF, Partridge JF, Genier S, Javerzat JP, Allshire RC (2001) Requirement of heterochromatin for cohesion at centromeres. Science 294: 2539-2542.
S2. Bernard P, Drogat J, Maure JF, Dheur S, Vaur S, Genier S, Javerzat JP (2006) A screen for cohesion mutants uncovers Ssl3, the fission yeast counterpart of the cohesin loading factor Scc4. Curr Biol 16: 875-881
S3. Bernard P, Schmidt CK, Vaur S, Dheur S, Drogat J, Genier S, Ekwall K, Uhlmann F, Javerzat JP (2008) Cell-cycle regulation of cohesin stability along fission yeast chromosomes. EMBO J 27: 111-121

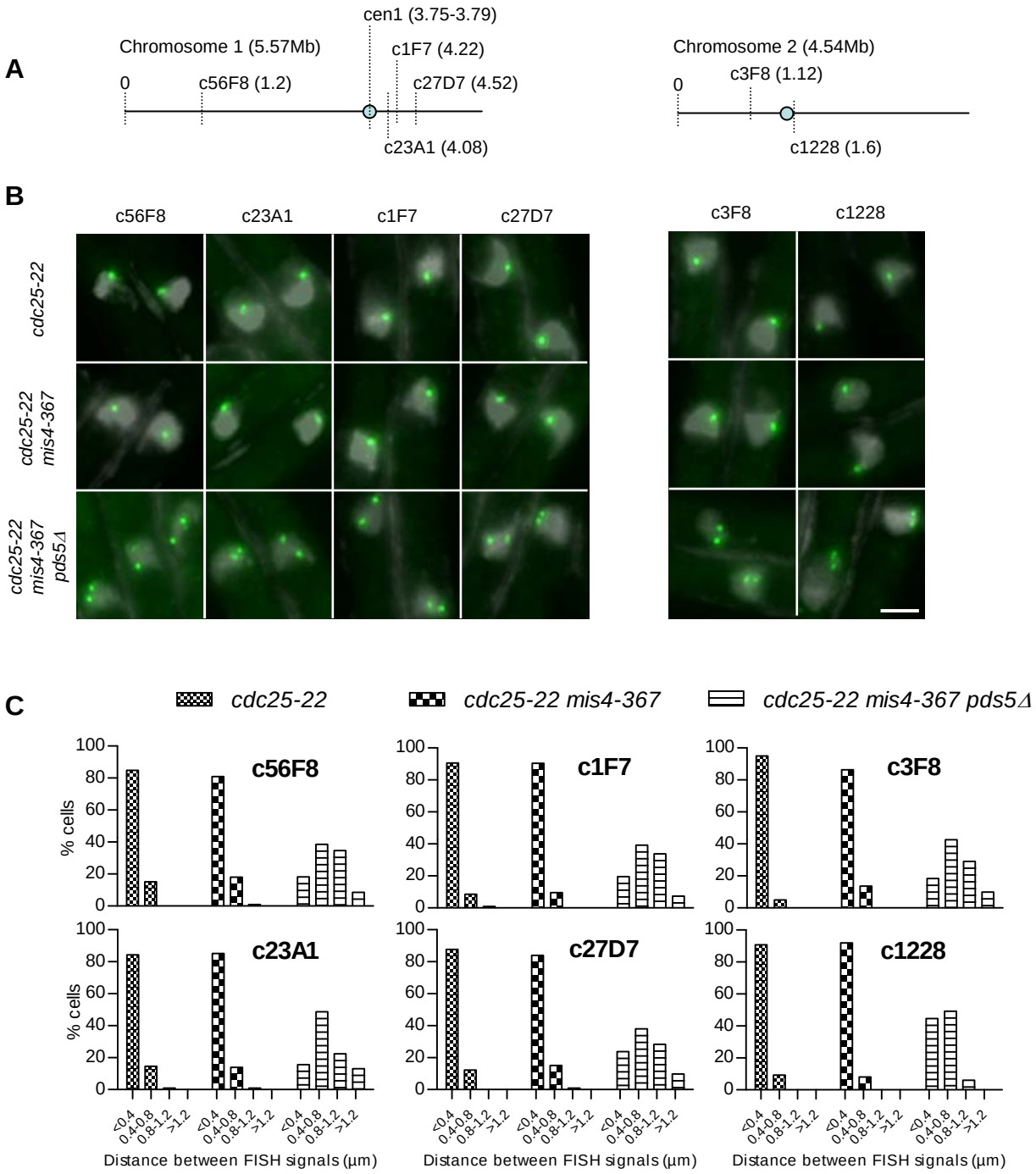

Figure S1. Loss of sister-chromatid cohesion in *pds5Δ* arrested G2 cells.
(**A**) Schematics showing the position of the FISH probes along chromosomes 1 and 2. Distances are in megabases. (**B**) FISH on G2 arrested cells. Cycling cells at 25°C (~80% G2) were shifted to 37°C for 3 hours and processed for FISH with the indicated cosmid probes. FISH signals appear in green, DAPI-stained nuclei in grey. Bar = 2µm. In an otherwise wt or *mis4-367* background the 2 FISH signals are co-localized or closely apposed to each other. By contrast the two FISH signals are separated in *pds5Δ* cells. (**C**) The distance between the 2 FISH signals was measured for 100-150 nuclei per sample. The distribution is similar in wt and *mis4-367* cells with most cells showing closely apposed (<0.4µm) signals. By contrast, most *pds5Δ* cells show widely separated (>0.4µm) FISH signals.

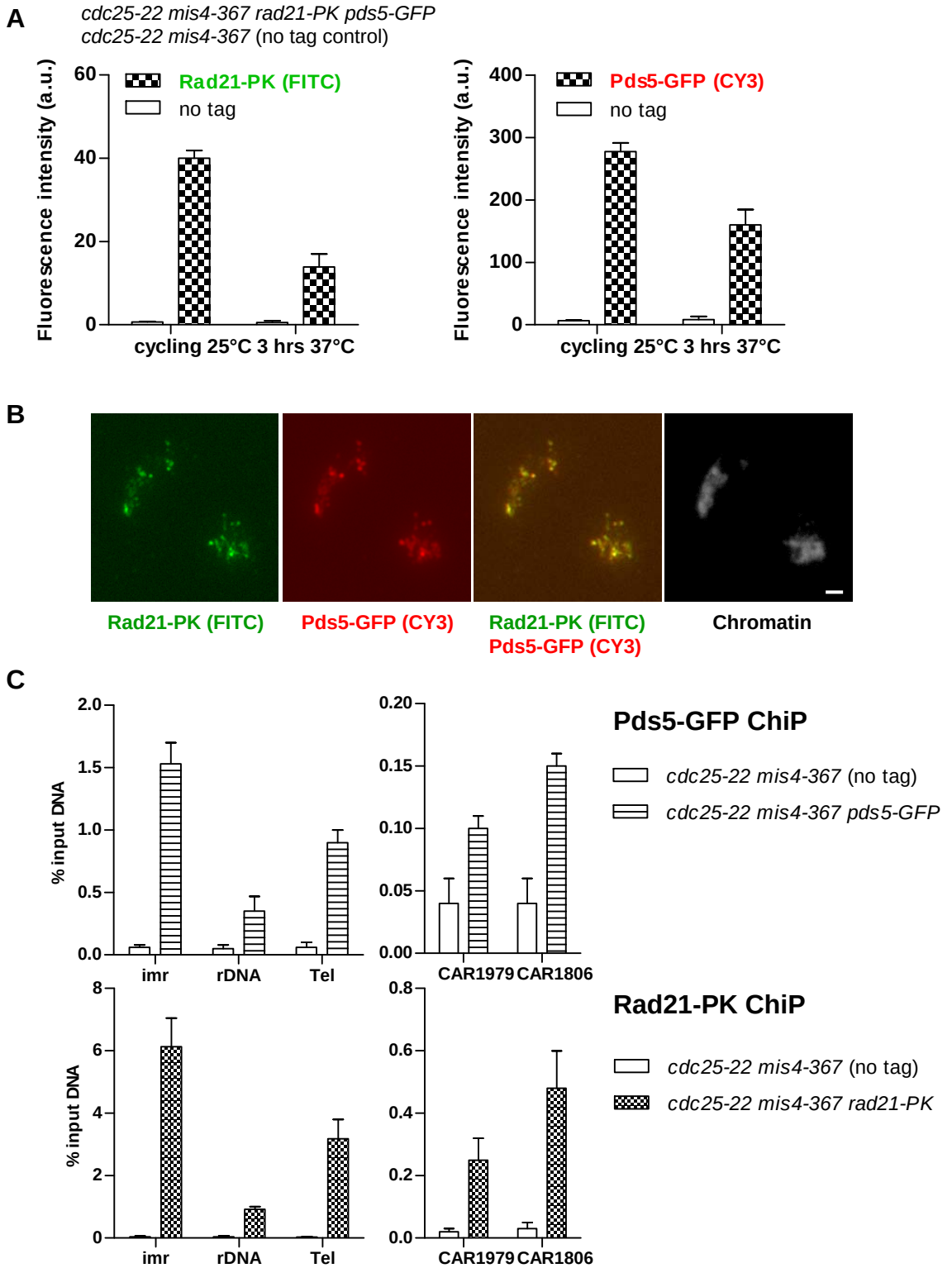

Figure S2. Pds5 co-localizes with the stable fraction of Rad21 on replicated chromosomes. (**A**) A fraction of Pds5 remains bound to G2 chromosomes after inactivation of the cohesin loader. Cycling *cdc25-22 mis4-367 rad21-PK pds5-GFP* cells were shifted to 37°C for 3 hours. Chromatin-bound Rad21-PK and Pds5-GFP were quantified from nuclear spreads before and after the temperature shift from 70-80 nuclei per sample. Error bar = 95% confidence interval of the mean with α=0.05. (**B**) Images of nuclear spreads after the 3 hours shift at 37°C showing that Pds5-GFP and Rad21-PK dots are co-localized. Bar = 2µm. (**C**) ChiP assay after the 3 hours shift at 37°C showing that Pds5-GFP and Rad21-PK display similar binding patterns. Error bar = SD from 3 ChiPs.

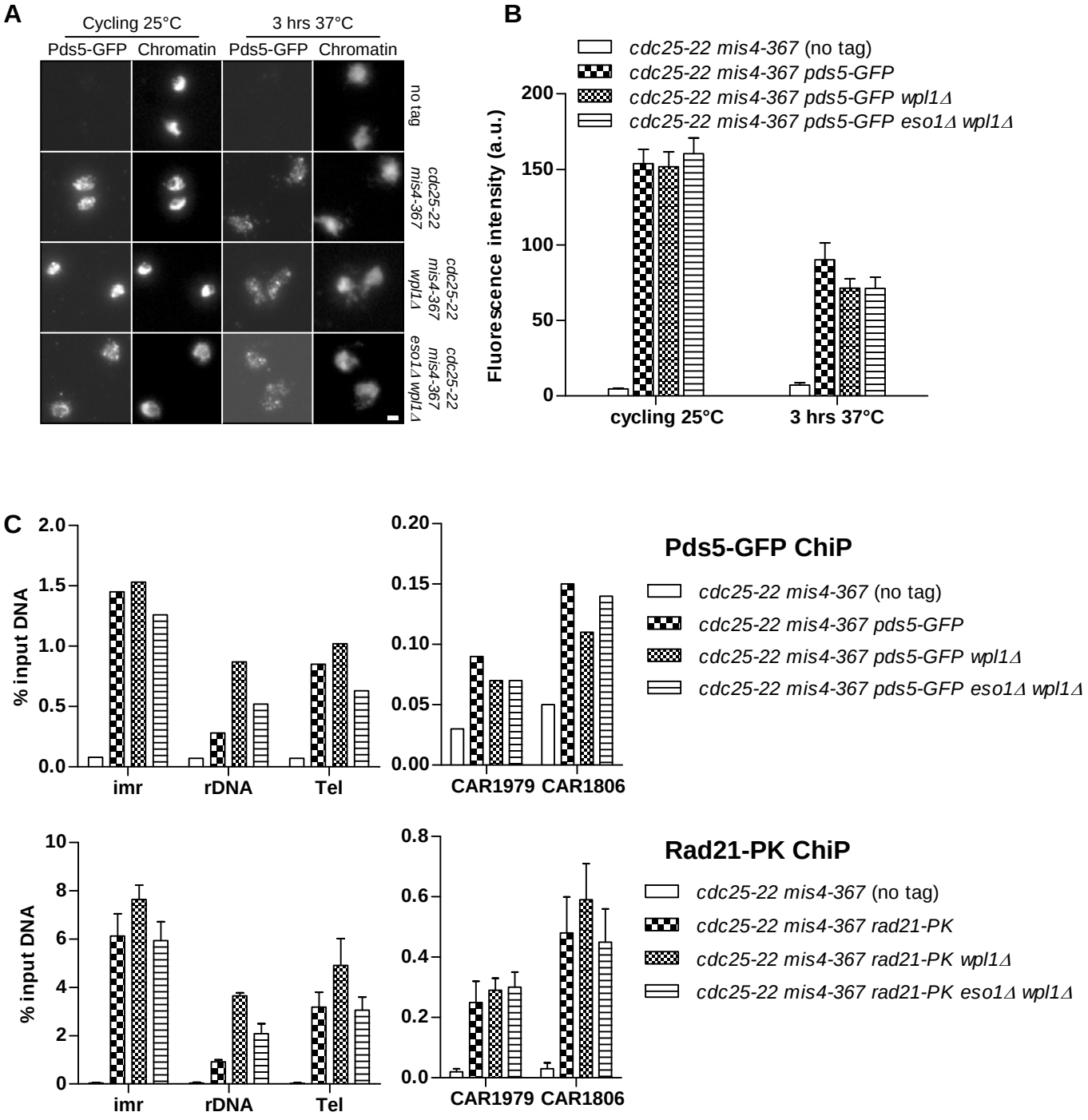

Figure S3. Pds5 and Rad21 binding to chromosomes in *wpl1Δ* and *eso1Δ wpl1Δ*.
Cycling cells at 25°C were shifted to 37°C for 3 hours to prevent further cohesin deposition (*mis4-367*) while *cdc25-22* prevented entry into mitosis. (**A**) Images of Pds5-GFP immunofluorescence on nuclear spreads from cells collected before and after 3 hours at 37°C. Chromatin was counterstained with DAPI. Bar = 2µm. (**B**) Quantification of chromatin-bound Pds5. Pds5-GFP fluorescence intensity was measured for 50-100 nuclei for each sample. Error bar = 95% confidence interval of the mean with α =0.05. (**C**) ChIP assays showing that Pds5 and the stable fraction of Rad21 are found at the same chromosomal locations. Cells were collected 3 hours after the shift at 37°C and processed for Pds5-GFP ChiP (mean from 2 ChiPs) and Rad21-PK ChiP (error bar = SD from 4 ChiPs).

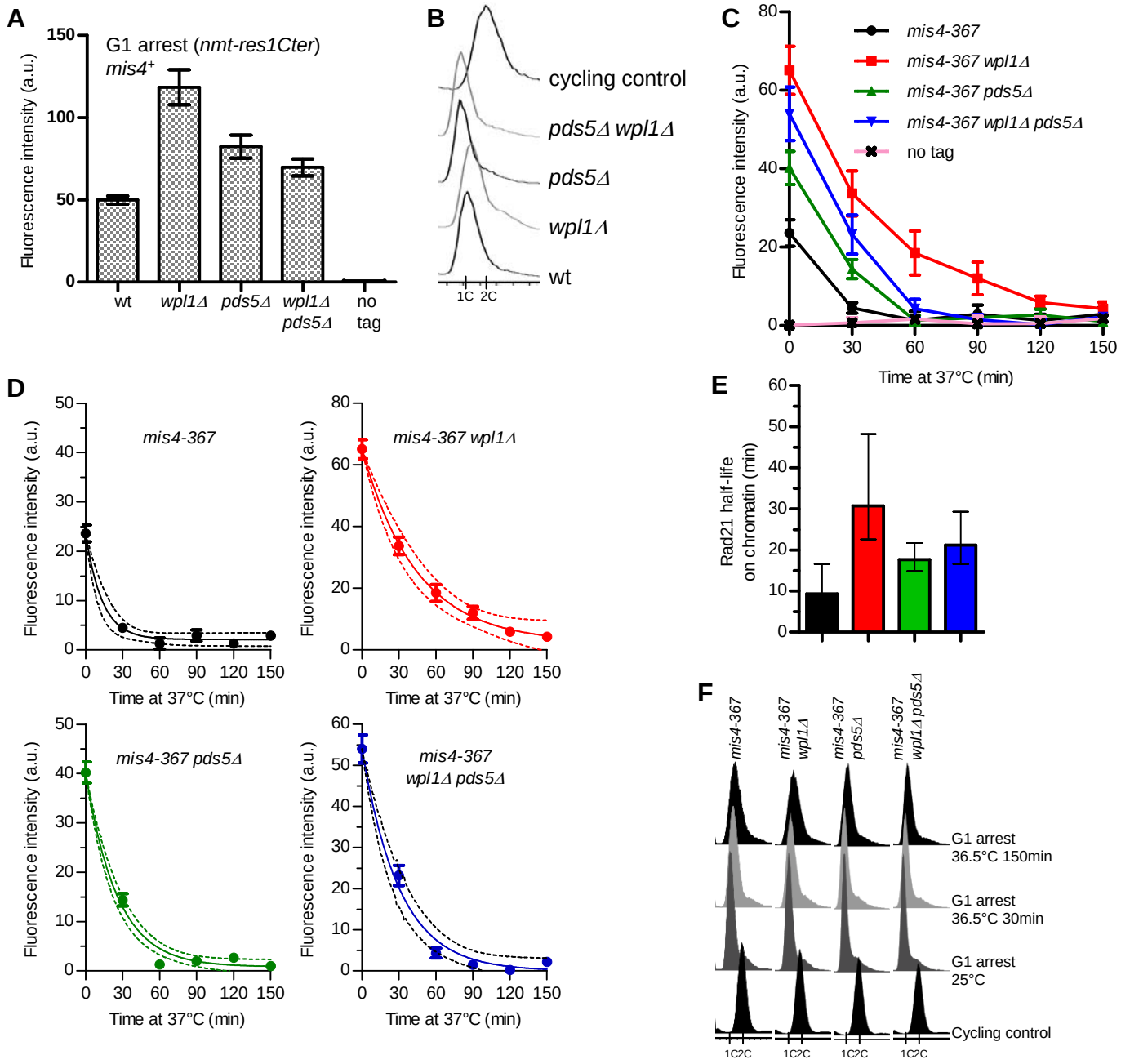

Figure S4. Wpl1 and Pds5 promote Rad21 release from G1 chromatin

(**A**) Steady state amount of chromatin-bound Rad21-PK in G1 arrested *mis4*$^{+}$ cells. Cells were arrested in G1 by the overexpression of the C-terminal domain of Res1 (*nmt-res1Cter* [S3]). Nuclear spreads were made and chromatin-bound Rad21-PK was detected by indirect immunofluorescence. Fluorescence intensity was measured for 50-100 nuclei per sample. Error bar = 95% confidence interval of the mean with α =0.05.(**B**) Flow cytometry analysis shows that cells arrested with a 1C DNA content. (**C**) Kinetics of Rad21 removal from G1 chromatin. Cells bearing the *mis4-367* mutation were arrested in G1 at 25°C as in (A) and then shifted to 36.5°C to prevent further cohesin loading. Rad21-PK fluorescence was measured from nuclear spreads at the indicated time-points (50-100 nuclei per sample). Error bar = 95% confidence interval of the mean with α =0.05.(**D**) The curves in (C) were fitted to a single exponential (one phase decay) to estimate Rad21 half-life on chromatin. Error bars = 95% confidence interval of the mean with α =0.05.The dotted lines show the 95% confidence bands. (**E**) Rad21 half-life on G1 chromatin. The error bars represent the 95% confidence intervals. (**F**) DNA content analysis showing that cells remained arrested with a G1 DNA content during the duration of the experiment.

The experiment in (A) indicates that the steady state amount of chromatin-bound Rad21 is increased in *wpl1Δ* and *pds5Δ* cells and the double-mutant behaves as *pds5Δ*, showing that *pds5Δ* is epistatic to *wpl1Δ*. This is consistent with Wpl1 and Pds5 acting in a common pathway that stimulates cohesin removal from chromatin. Loss of Pds5 may slightly alter the stability of cohesin binding to DNA, resulting in a lower steady-state.

A similar relationship between Wpl1 and Pds5 was deduced from the kinetics of Rad21 removal from chromatin upon inactivation of the cohesin loader (C). Rad21 half-life on chromatin (E) is extended in *wpl1Δ* and to a lesser extent in *pds5Δ* and *pds5Δ* is epitastic to *wpl1Δ*.

It is of note that the deletion of *wpl1* or *pds5* slows-down the rate of cohesin release but does not lead to the full stabilization of cohesin onto chromatin.

Table S1. Strains used in this study

	Strain	Genotype
Figure 1A	3678	*h⁻ ura4 psm3-GFP-nat^R*
	3469	*h⁻ ura4 psm3-GFP-ura4⁺ wpl1Δ::kan^R eso1Δ::ura4⁺*
	3505	*h⁻ ura4 psm3-GFP-ura4⁺ wpl1Δ::kan^R*
	3676	*h⁻ ura4 psm3-GFP-nat^R pds5Δ::ura4⁺*
Figure 1B	2	*h⁻*
	2967	*h⁻ ura4 pds5Δ::ura4⁺*
Figure 1C	2	*h⁻*
	3738	*h⁻ pds5Δ::nat^R*
	5415	*h⁻ pds5Δ::nat^R clr6-1*
	5505	*h⁻ clr6-1*
Figure 2	405	*h⁻ cdc25-22*
	3448	*h⁻ cdc25-22 rad21-9PK-kan^R*
	5687	*h⁺ cdc25-22 rad21-9PK-kan^R pds5Δ::ura4⁺ ura4*
Figure 3	405	*h⁻ cdc25-22*
	3202	*h⁻ cdc25-22 mis4-367*
	3333	*h⁻ cdc25-22 mis4-367 rad21-9PK-kan^R*
	3378	*h⁻ cdc25-22 mis4-367 rad21-9PK-kan^R pds5Δ::ura4⁺ ura4*
Figure 4	3202	*h⁻ cdc25-22 mis4-367*
	3333	*h⁻ cdc25-22 mis4-367 rad21-9PK-kan^R*
	3355	*h⁻ cdc25-22 mis4-367 rad21-9PK-kan^R wpl1Δ::kan^R*
	3378	*h⁻ cdc25-22 mis4-367 rad21-9PK-kan^R pds5Δ::ura4⁺ ura4*
	3385	*h⁻ cdc25-22 mis4-367 rad21-9PK-kan^R wpl1Δ::kan^R pds5Δ::ura4⁺ ura4*
Figure 5	3202	*h⁻ cdc25-22 mis4-367*
	3726	*h⁻ cdc25-22 mis4-367 rad21-9PK-kan^R wpl1Δ::hyg^R eso1Δ::ura4⁺ ura4*
	4513	*h⁻ cdc25-22 mis4-367 rad21-9PK-kan^R pds5Δ::ura4⁺ eso1Δ::ura4⁺ ura4*
	4514	*h⁻ cdc25-22 mis4-367 rad21-9PK-kan^R wpl1Δ::hyg^R pds5Δ::ura4⁺ eso1Δ::ura4⁺ ura4*
Figure S1	405	*h⁻ cdc25-22*
	3202	*h⁻ cdc25-22 mis4-367*
	6029	*h⁻ cdc25-22 mis4-367 pds5Δ::ura4⁺ ura4*
Figure S2	3202	*h⁻ cdc25-22 mis4-367*
	3333	*h⁻ cdc25-22 mis4-367 rad21-9PK-kan^R*
	3492	*h⁻ cdc25-22 mis4-367 pds5-GFP-kan^R*
	4818	*h⁻ cdc25-22 mis4-367 pds5-GFP-kan^R rad21-9PK-kan^R*
Figure S3	3202	*h⁻ cdc25-22 mis4-367*
	3492	*h⁻ cdc25-22 mis4-367 pds5-GFP-kan^R*
	3513	*h⁻ cdc25-22 mis4-367 pds5-GFP-kan^R wpl1Δ::kan^R*
	5721	*h⁻ cdc25-22 mis4-367 pds5-GFP-kan^R wpl1Δ::hyg^R eso1Δ::ura4⁺ ura4*
Figure S4 A-B	2760	*h⁻ ura4⁺-nmt-res1Cter*
	3330	*h⁻ ura4⁺-nmt-res1Cter rad21-9PK-kan^R*
	3332	*h⁻ ura4⁺-nmt-res1Cter rad21-9PK-kan^R wpl1Δ::kan^R*
	3379	*h⁻ ura4⁺-nmt-res1Cter rad21-9PK-kan^R pds5Δ::ura4⁺*
	3412	*h⁻ ura4⁺-nmt-res1Cter rad21-9PK-kan^R wpl1Δ::kan^R pds5Δ::ura4⁺*
Figure S4 C-F	2760	*h⁻ ura4⁺-nmt-res1Cter*
	3324	*h⁻ ura4⁺-nmt-res1Cter mis4-367 rad21-9PK-kan^R wpl1Δ::kan^R*
	3328	*h⁻ ura4⁺-nmt-res1Cter mis4-367 rad21-9PK-kan^R*
	3357	*h⁻ ura4⁺-nmt-res1Cter mis4-367 rad21-9PK-kan^R pds5Δ::ura4⁺*
	3413	*h⁻ ura4⁺-nmt-res1Cter mis4-367 rad21-9PK-kan^R wpl1Δ::kan^R pds5Δ::ura4⁺*